

Features of magnetosphere-ionosphere coupling during breakups and substorm onsets inferred from multi-instrument alignment

I. Voronkov, A. Runov, A. Koustov, K. Kabin, M. Meurant, E. Donovan, C. Bryant, and E. Spanswick

Abstract: We consider a sequence of activations which include pseudo-breakups, small local substorms, and a full substorm using a fortunate multi-instrument coverage between 0300 and 0700 UT on September 15, 2001. For this period of time, there was a radial alignment of GOES, and Cluster ($\sim 19 R_E$) in the near-midnight magnetotail mapped to the Canadian sector covered by the IMAGE field of view along with fully functional hi-resolution photometers, and magnetometers. This allows reasonable featuring of auroral breakup and substorm onset components as they are observed both in the magnetosphere and ionosphere. In this paper, we concentrate on general description and relative timing of the auroral breakup signatures, dipolarization and onset of Pi pulsations at geostationary orbit, and large (up to 1000 km/s) tailward flows and strong bipolar variations in the central plasma sheet. This paper is meant to complement the accompanying paper [10].

Key words: Breakup, Onset, Substorm.

1. Introduction

In a substorm onset problem, one of the central issues is the inter-scale interactions of various regions. These include processes in the near-Earth plasma sheet (NEPS) and the auroral intensification and current formation in the ionosphere, processes in the near-Earth breakup region and in the mid-tail reconnection region, and coupling of the central plasma sheet (CPS) and ionosphere at onset.

In studying the essential relations between the substorm onset components, significant successes have been recently achieved in both micro-scale analysis of plasma sheet processes and global picturing of the magnetosphere-ionosphere coupling using multi-instrument alignments. Some observations indicate that onset is an interactive process involving the near-Earth breakup and mid-tail reconnection. It has been suggested that the near-Earth breakup is associated with some sort of the interchange instability, most probably a drift ballooning mode, leading to a current disruption at roughly $6-10 R_E$, whereas reconnection is presumably a result of the Hall effect in the very thin, and sometimes bifurcated, current sheet at larger radial distances. The most disputed mechanisms of interaction between these two processes, or triggering one another, are rarefaction or compressional waves propagating from the NEPS to the CPS and earthward bursty flows from the reconnection region to the NEPS. For reference purposes, we overview sev-

eral recent observation-based studies which also provide more complete list of literature on the subject.

A drift ballooning instability in the NEPS was observed by Wind [3] and CRRES [5] and the spatial and temporal characteristics of unstable modes are in agreement with nonlinear auroral vortex formation at breakups [13]. In the more distant plasma sheet, thin and bifurcated current sheet was detected by Cluster [2], [9]. The Hall current structure at the reconnection region was observed by Geotail [6] and Cluster [1] providing support for the Hall reconnection model being a likely mechanism for the mid-tail reconnection.

Perhaps the most challenging problem is to detect a mechanism which provides an interaction between these regions. Presumably, this interaction can proceed in both ways, earthward and tailward, and even as a simultaneous collapse of the entire plasma sheet (PS). Roux et al. [8] identified azimuthally propagating waves seen by Cluster in a mid-tail region as a result of a ballooning or another local instability which is able to reduce or interrupt a cross tail current. They suggested that in series, these local processes can result in a global CPS current reduction and dipolarization. In contrast, using a radial alignment of Cluster and ISTP, Sergeev et al. [11] interpreted onset as earthward-contracting reconnected tube produced by impulsive reconnection in the mid-tail PS. On the other hand, some substorms are initiated by bursty bulk flows, presumably launched from the reconnection regions and propagating earthward (see, e.g., [7] and references therein). The near-Earth breakup triggering by bursty flows is the subject of discussions but some recent observations and modeling suggest that compressional waves may provide an energy transport channel from the flow braking region to the NEPS (e.g., [4], [12], [14]).

In this study, we attempt to use a fortunate alignment of Cluster, GOES, IMAGE, and Canadian ground based instruments to investigate sequences of substorm onset signatures in the system of NEPS, mid-tail PS, and auroral ionosphere. The detailed local Cluster observations and their analysis for

Received 14 June 2006.

I. Voronkov, M. Meurant, E. Donovan, C. Bryant, and E. Spanswick. Dpt. of Physics and Astronomy, University of Calgary, Calgary, AB, T2N 1N4, Canada

A. Runov. Space Research Institute, Austrian Academy of Sciences, Schmiedlstrasse 6, A-8042, Graz, Austria

A. Koustov. Dpt. of Physics and Engineering, University of Saskatchewan, 116, Science Place Saskatoon, SK, S7N 5E2, Canada

K. Kabin. Dpt. of Physics, University of Alberta, Edmonton, AB, T6G 2J1, Canada

this event are described in the accompanying paper [10]. Here, we concentrate on the temporal and spatial description of onsets in a more global context of the ionosphere-magnetosphere system.

2. Observations on September 15, 2001

During the time interval from 0100 through 0630 UT on September 15, 2001, Cluster was, for the most part, in the night-side central plasma sheet. During the interval of 0330-0630 UT, several auroral activations (from small PSBs to a full substorm) were registered over the Canadian sector bracketed by two geostationary satellites, GOES 8 and GOES 10. The Cluster barycenter position was $(-18.9, 3.7, -1.9) R_E$ at 0400 UT and $(-18.5, 3.3, -3.4) R_E$ at 0600 UT. The IMAGE satellite observed auroral emissions for the entire interval over the Canadian sector. This provides a unique opportunity to use this conjunction of Cluster, IMAGE, GOES, CANOPUS, and NR-Can facilities for studying substorm processes, namely to correlate mid-tail and ground-based signatures of different substorm stages. Mapping of Cluster, IMAGE, and GOES with respect to ground-based stations is illustrated by Figure 1.

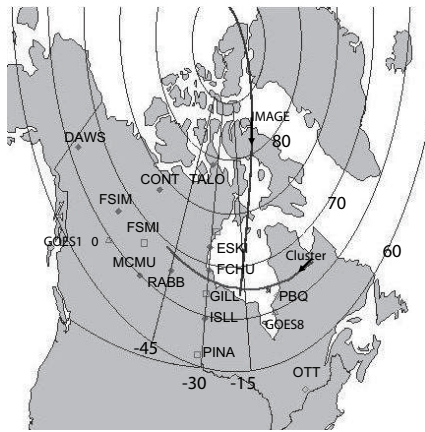


Fig. 1. Locations of NORSTAR, CANOPUS, and NRCan observatories along with ionospheric footprints of the Cluster, IMAGE, and GOES 8 and 10 satellites.

Good quality meridian scanning photometer (MSP) data obtained at Forth Smith and Gillam, including high-resolution data at Gillam, position of IMAGE capturing the Canadian sector, available data from Cluster, and high resolution GOES data bring events during this interval of time to a great spot of interest.

The entire data set used for this study can be outlined as follows. WIND and Geotail were used to monitor solar wind (SW) parameters. IMAGE provided global auroral imaging of the Canadian sector. This was used to identify the position of onset and its further temporal and spatial dynamics (e.g., vortex and surge formation and propagation). With the global framework provided by IMAGE, the fine structure of auroral dynamics can be revealed using higher-resolution optical data from MSPs. Cluster observations showed the dynamics of the near-midnight plasma sheet at roughly $19 R_E$ down the tail.

GOES spacecraft provided timing for dipolarization and onset of Pi2. Finally, the overall picture of disturbances was monitored by the CANOPUS and NRCan magnetometers.

3. Pre-history and the growth phase

Prior to the period of the immediate interest for this study, there was a large substorm which started after 2330 UT on September 14, 2001 and ended at roughly 0145 UT on September 15, 2001. This was the latest noticeable perturbation prior to activations between 0340 and 0630 UT, which are focused in this study. After 0100 UT, the IMF B_z was dominantly northward until ~ 0335 UT when the sharp negative turning started. Other SW parameters (B_y , N , P , V) also showed rather smooth variations during that time as illustrated in Figure 2 showing B_y , B_z , and V_x measured by Geotail traveling approximately at $(10, 15, 1.5) R_E$. Geotail and WIND data closely followed each other suggesting that the SW parameters were homogeneous on the scale size of the Earth magnetosphere.

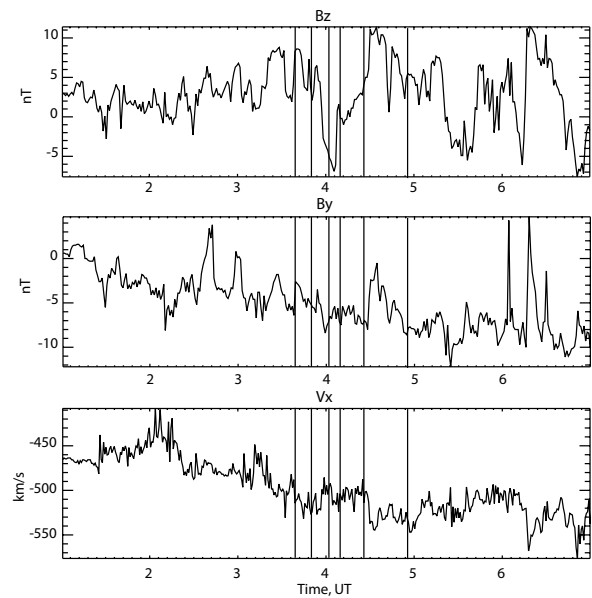


Fig. 2. IMF B_z and B_y and solar wind V_x components as measured by the Geotail. Vertical lines indicate times of onsets.

After 2350 UT, GOES 8 registered very strong stretching of field lines with the maximum of $H_e/H_p \sim 2$. It gradually reduced to ~ 1.5 after 0200 UT and stayed at this level until the first dipolarization occurred at 0339 UT. During this interval, GOES 10 was in the near-dipolar field region and magnetic field variations at the satellite location were very smooth.

After ~ 0100 UT, Cluster was in the central PS and observed no significant disturbances until the first intensification at 0338-0340 UT. During this interval, B_z gradually decreased, indicating stretching. Also, the post-substorm (after 0100 UT) PS can be characterized as rather "hot" with the proton temperature around 10 keV (which is high but not anomalous). The Cluster summary plot is shown in Figure 3. For more data plots and detailed discussion, see [10] in this issue.

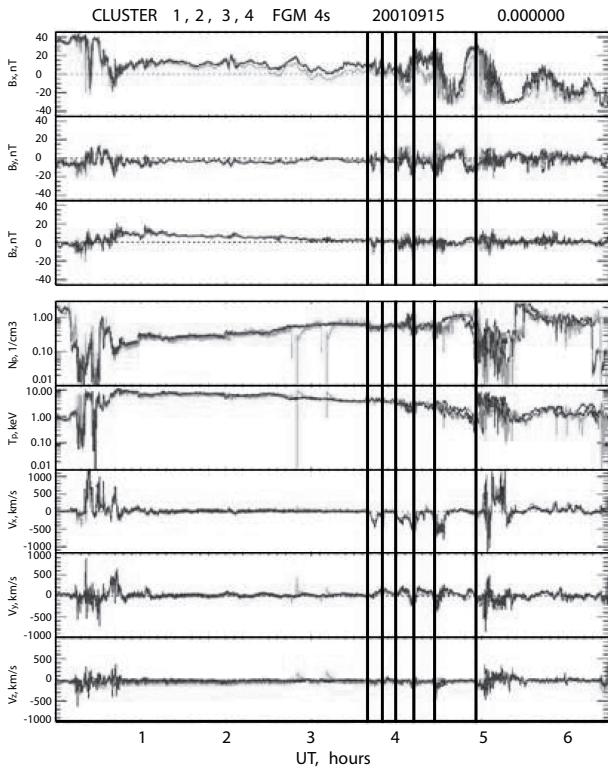


Fig. 3. The Cluster summary plot. Vertical lines indicate times of onsets.

The magnetic field perturbation in the Canadian sector recovered after 0100 UT and remained quiet until the first onset at 0338-0340 UT. Also according to IMAGE, the auroral zone was also very quiet and dim after 0100 until onset at 0338 UT.

The growth phase timing is quite uncertain for this event, mostly due to the lack of any pronounced signatures in the solar wind. One could even argue there was a growth phase at all. We will simply describe variations, which can be considered as growth phase signatures. Cluster showed continuous field line stretching. According to the Gillam MSP, equatorward motion of auroras started after roughly 0220-0230 UT and continued until 0340 UT. At the late growth phase, IMAGE registered dimming and virtually disappearance of the oval in both electron and proton auroras which also can be attributed to significant stretching of the magnetotail. No any other significant variations were registered until onset at 0339 UT.

All these observations for the post-substorm period of time (~0100-0335 UT) suggest that the magnetosphere-ionosphere system was in a stationary state free of any noticeable disturbances. At the same time, the plasma sheet was at a fairly high energy level, quite stretched and hot. Presumably, this was the main background condition for the active period discussed below. The growth phase was not too pronounced for this event. The main signatures can be interpreted as continuous stretching of the entire plasma sheet.

4. Onset positions and timing

Large scale optical onset positions and timing were defined using the IMAGE WIC data with temporal resolution of 2 min. According to IMAGE (Figure 4), the first five onsets prior the main substorm (at 0455 UT) occurred in a longitudinal sector monitored by the Canadian MSPs and magnetometers. High resolution ground-based measurements allowed us to study dynamics of disturbances in greater details. Sample data from magnetometers encountering the activation region and GILL MSP are shown in Figure 5 (CANOPUS) and Figure 6 (NR-Can). In this section, only these five activations are targeted whereas the last more eastward substorm onset will be considered separately. Because all five onsets occurred close to the GILL MSP, we used high-resolution MSP data to find times and longitudinal positions of auroral breakups (Figure 7). GOES 8 (Figure 8) provided the timing of dipolarization.

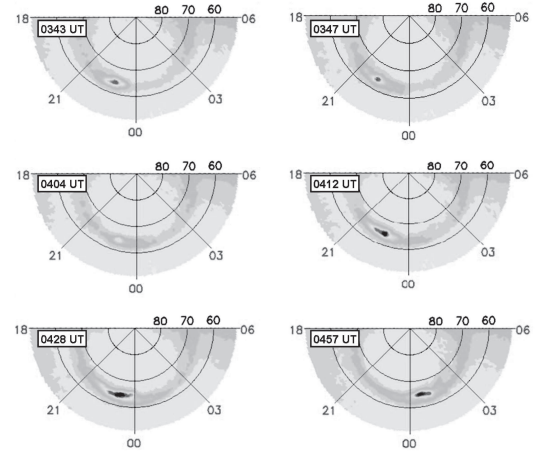


Fig. 4. IMAGE WIC snapshots at onsets.

4.1. Timing

From analysis of GOES 8 data for these activations, we concluded that dipolarization and $Pi2$ at geostationary orbit represent the most reliable signatures of onset. Analyzing all other data described above, the following timing of observed features with respect to the moment of dipolarization (taken as $t = 0$ min) has been revealed. Time is given in minutes with respect to dipolarization at $t = 0$ (e.g., -6 means 6 min prior to dipolarization, or : 1 stands for 1 min after dipolarization)

#1 (0339 UT):

- 6: Equatorward auroral precursor;
- 0: Dipolarization and $Pi2$ at GOES, GBO breakup;
- 1: GBO $Pi2$ and magnetic bay;
- 2: Onset seen by IMAGE, tailward flow and bipolar variation of the magnetic field at Cluster;
- 5: The maximum tailward flow seen at Cluster.

#2 (0350 UT):

- 3: GBO and IMAGE auroral breakup.
- 0: $Pi2$ and dipolarization at GOES, magnetic bay at PBQ, fast tailward flow and bipolar magnetic fluctuations at Cluster.

#3 (0402 UT):

- 3: Tailward flow and bipolar variations at Cluster;

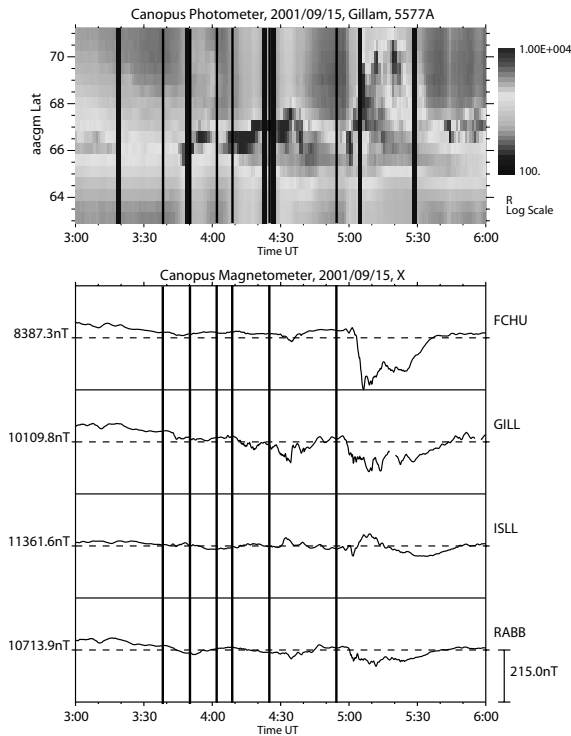


Fig. 5. Summary plot of Gillam MSP observations (sampling data are used) and magnetic field X-component variations at a number of CANOPUS sites. Black vertical lines indicate times of onsets.

0: Pis and dipolarization at GOES, GBO and IMAGE breakup, GBO magnetic bay, very strong magnetic field oscillations at Cluster.

#4 (0409 UT):

-2: Northward turning of the B_Z IMF, start of bipolar variations at Cluster;

0: Pi and dipolarization at GOES, tailward flow at Cluster;

2-3: GBO and IMAGE optical breakup, GBO magnetic bay;

3-4: westward travelling surge (WTS), maximum of the tailward flow at Cluster.

#5 (0425 UT):

-1: auroral breakup;

0: Pis and dipolarization at GOES, GBO magnetic onset;

1: Onset detected by IMAGE, Cluster registered a tailward flow, growth of the proton temperature, and bipolar variations;

3: Fully developed WTS and electrojet;

4.2. Position of auroral onset

As seen from IMAGE data (Figure 4), all five onsets occurred at longitudes close to the Churchill line. This allows us to use the Gillam MSP data in order to identify the latitudinal positions of the activations. For this purpose, we analyzed the high-resolution data (Figure 7).

The first two intensifications could have been treated as one local substorm with double onset (or pseudo-breakup and onset) from the point of view of the GBO, IMAGE, and geostationary observations. However, Cluster registered two distinct tailward flow bursts accompanied by the B_Z reversals (see [10] for details).

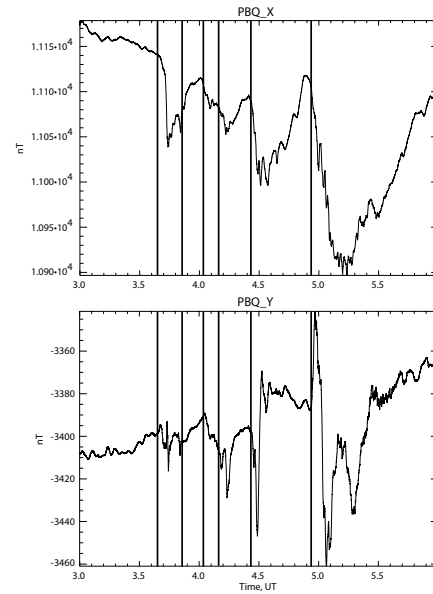


Fig. 6. PBQ magnetic data used for the electrojet and Pi2 onset timing. Black vertical lines indicate times of onsets.

The first activation started in a rather typical way (Figure 9): equatorward auroral precursor intensified ~ 6 min prior to onset (0333 UT) and led to auroral breakup (PSB) at the poleward edge of the proton aurora band (0339 UT), with some latitudinal expansion at onset.

This first PSB at the equatorward boundary developed into full onset (activation #2) with much stronger brightening and noticeable poleward expansion after 0347 UT roughly 3 min prior to other onset signatures. This brightening was also seen in IMAGE data. Since the previous activity did not move too far northward from the origin, this activation still started at the equator-most aurora.

Activation #3 commenced in a similar way to the first one with aurora intensification at the equatorward edge at 0402 UT. In this case, it happened virtually at the same time as onset was registered by GOES, PBQ, and IMAGE. However, the further dynamics was quite different. When the auroral activation began saturating (0408-0410 UT), a sharp northward gradient of the IMF B_Z close to magnetopause was detected by Geotail. Perhaps, this caused activation #4 which can be considered as triggered continuation of the previous one and developed into a quite pronounced, though still rather local, substorm. Unlike previous three activations, it started from the most active region (remaining from activation #3) quite poleward from the equatorward boundary of the auroral zone marked by the proton aurora band. This optical onset was simultaneously observed by the GILL MSP and IMAGE with a delay of 2-3 minutes of onset at geostationary orbit.

Activation #5 started in the same way as #4: at the time of onset at geostationary orbit (slightly preceding it), the most active region from the previous substorm intensified and resulted in a fully developed WTS 3-4 minutes later. Again, this onset occurred poleward from the equatorial boundary and proton aurora band.

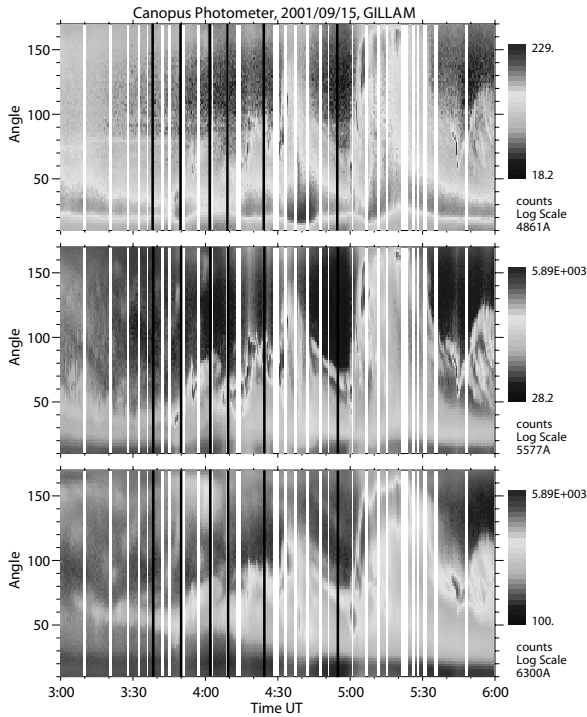


Fig. 7. Summary plots of GILL high resolution MSP. Black vertical lines indicate times of onsets.

5. Full substorm onset features

The first signatures of onset were detected as the magnetic bay and Pi commencement at PBQ (0454 UT) and the Pi onset at OTT (pulsations lasted until 0525 UT). Lower frequency (2 min) pulsations and strong variations in Z also started at PBQ and lasted until 0515 UT. The magnetic signatures were delayed at the Churchill line owing to the westward propagation of the disturbances from their more eastbound origin. Preceding the onset, Cluster measurements showed a thin (half thickness on the order of 3000 km) and bifurcated plasma sheet. At the time of 0455-0502 UT, Cluster registered very strong (up to 25 nT) oscillations (which can be interpreted as a kinking mode [10]) of the magnetic field on the background of the large B-gradient and azimuthal duskward motion of the current sheet [10].

Optical onset was registered by IMAGE at 0457 UT in the post-midnight sector. Figure 10 provides key snapshots of WIC during the entire event.

Due to the position of onset, the optical signatures of the surge reached Gillam only at 0459 UT, as seen in high resolution MSP (Figure 8). After that, the surge showed significant poleward expansion (at 0459-0506 UT) in a "jump-like" manner. Also owing to the eastward location of onset, the dipolarization at GOES 8 did not start until 0500 UT.

After 0500 UT, the current sheet became very dynamic. At 0459-0501 UT, Cluster registered a pulse of tailward and duskward bulk flow (roughly up to 200 km/s). Following this at 0501-0502 UT, Cluster showed a sharp growth in the proton energy roughly from 1 to 10 keV where it stayed for a long while. This growth was accompanied by the earthward bulk of high energy (more than 10 keV) protons. At that time (0501-

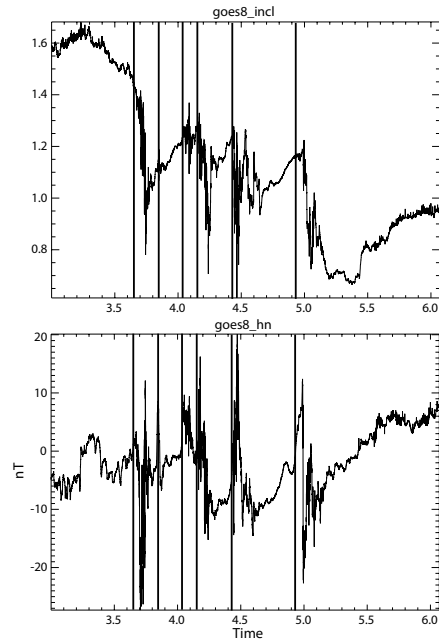


Fig. 8. Magnetic field inclination (representing dipolarizations) and H_n component (illustrating onsets of Pi) as detected by GOES 8. Black vertical lines indicate times of onsets.

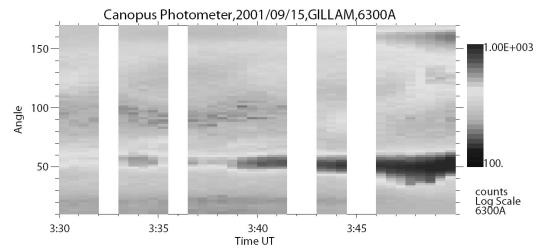


Fig. 9. 630 nm high resolution MSP data for activation 1 (white lines indicate periods with no data).

0504 UT) a very thin (half-thickness less than 1000 km) current sheet was detected.

During this period of time, the ground-based instruments registered further expansion of the activation. At 0501 UT, brightening and poleward expansion began at FSMI, which is in agreement with the IMAGE data. At 0502 UT, the main substorm bay started at FCHU and a current loop formed above GILL indicating large expansion of the electrojet.

Following this, at 0503-0505 UT, the surge reached its greatest magnitude and poleward expansion. As seen from IMAGE and MSP data, the high latitude portion of the surge brightens dramatically at this time (whereas the equatorward activity recovered). This was the time when Cluster detected a sharp reversal of the bulk flow from tailward to Earthward of the magnitude up to 800 km/s. Analysis of Cluster data indicates that variations of plasma parameters are consistent with signatures of the Hall reconnection in the CPS. After 0506-0507 UT, a double oval was seen by the GILL MSP and IMAGE (Figure 10), and the largest magnitude in the magnetic bay was registered above FCHU.

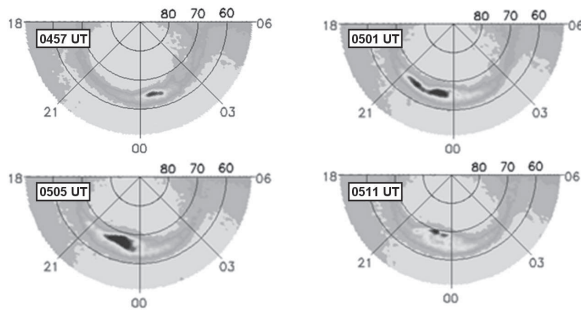


Fig. 10. IMAGE snapshots of the auroral breakup (0457 UT), surge formation (0501 UT), full substorm onset vortex (0505 UT), and double oval at the beginning of the recovery phase (0511 UT).

After roughly 0511 UT, the recovery phase signatures were observed in all main substorm components.

6. Conclusions and assertions

Owing to good longitudinal alignment of ground based and satellite observations, five activations, including local substorms and pseudo-breakups, on September 15, 2001 were used to infer onset features and their relative timing in the plasma sheet and ionosphere. The main results can be summarized as follows.

1. The most robust and repeatable features of onsets were dipolarization and onset of Pis in the near-Earth plasma sheet. We used this time-point as "the time of onset".

2. Auroral breakup can start from the precursor at the equatorial boundary of the auroral zone (which is more typical for isolated activations) as well as from most active regions which remain from the previous substorm quite poleward of the equatorial auroral boundary matching the proton aurora band.

3. Near-Earth breakups (including pseudo-breakups) were associated with strong tailward bursty flows (up to 1200 km/s) and large bipolar variations of the magnetic field.

4. For these activations, all signatures of onsets, from the NEPS to CPS and from the magnetosphere to the ionosphere, were seen within the time frame of 2-3 minutes.

Full substorm can be interpreted as a double onset event. The first one occurred in a similar way as the near-Earth breakups discussed above. The second led to a much larger substorm with fully developed WTS and electrojet. This onset was observed by Cluster at $19 R_E$ as a sharp reversal of the flow and other signatures which allow us to interpret it as the Hall-type reconnection. In the ionosphere, the large-scale vortex on the spatial scale of the auroral oval width was observed. These features followed by the formation of a double oval.

Acknowledgements

The CANOPUS and NORSTAR arrays are ground-based facilities funded by the Canadian Space Agency. We acknowledge NASA/GSFC, CDAWeb, and DARTS/Geotail data providers. We thank H. Singer for providing high resolution GOES 8 and GOES 10 data. The IMAGE FUV investigations were supported by NASA through SWRI subcontract. Poste-de-la-Baleine and Ottawa magnetic stations are funded and operated by The Geological Survey of Canada (National Resources of Canada). We thank A. Balogh for providing

Cluster FGM data and H. Reme for providing Cluster CIS data. This research was supported by the Natural Sciences and Engineering Research Council of Canada (NSERC) and the Canadian Space Agency.

References

1. Alexeev, I. V., C. J. Owen, A. N. Fazakerley, A. Runov, J. P. Dewhurst, A. Balogh, H. Rème, B. Klecker, and L. Kistler, Cluster observation of currents in the plasma sheet during reconnection, *Geophys. Res. Lett.*, **32**, L03101, 2005.
2. Asano, Y., R. Nakamura, W. Baumjohann, A. Runov, Z. Vörös, M. Volwerk, T. L. Zhang, A. Balogh, B. Klecker, and H. Rème, How typical are atypical current sheets? *Geophys. Res. Lett.*, **32**, L03108, 2005.
3. Chen, L.-J., A. Bhattacharjee, K. Sigsbee, G. Parks, M. Fillingim, and R. Lin, Wind observations pertaining to current disruption and ballooning instability during substorms, *Geophys. Res. Lett.*, **30**, 1335, 2003.
4. Kepko, L., M. G. Kivelson, and K. Yumoto, Flow bursts, breaking, and Pi2 pulsations, *J. Geophys. Res.*, **106**, 1903, 2001.
5. Kozelova, T. V., L. L. Lazutin, B. V. Kozelov, N. Meredith, and M. A. Danielides, Alternating bursts of low energy ions and electrons near the substorm onset, *Ann. Geophys.*, 2006, accepted.
6. Nagai, T., I. Shinohara, M. Fujimoto, S. Machida, R. Nakamura, Y. Saito, and T. Mukai, Structure of the Hall current system in the vicinity of the magnetic reconnection site, *J. Geophys. Res.*, **108**, 1357, 2003.
7. Nakamura, R., W. Baumjohann, R. Schödel, M. Brittnacher, V. A. Sergeev, M. Kubyshkina, T. Mukai, and K. Liou, Earthward flow bursts, auroral streamers, and small expansions, *J. Geophys. Res.*, **106**, 10,791, 2001.
8. Roux, A., O. Le Contel, D. Fontaine, P. Robert, P. Louarn, J.A. Sauvaud, and A.N. Fazakerley, Substorm theories and Cluster multi-point measurements, *ICS8 proceedings*, this issue, 2006.
9. Runov, A., R. Nakamura, W. Baumjohann, T. L. Zhang, M. Volwerk, H.-U. Eichelberger, and A. Balogh, Cluster observation of a bifurcated current sheet, *Geophys. Res. Lett.*, **30**, 1036, 2003.
10. Runov, A., I. O. Voronkov, Y. Asano, W. Baumjohann, R. Nakamura, M. Volwerk, A. Balogh and H. Reme, Cluster observations during pseudo-breakups and substorms, *ICS8 proceedings*, this issue, 2006.
11. Sergeev, V. A., M. V. Kubyshkina, W. Baumjohann, R. Nakamura, O. Amm, T. Pulkkinen, V. Angelopoulos, S. B. Mende, B. Klecker, T. Nagai, J.-A. Sauvaud, J. A. Slavin, and M. F. Thomsen, Transition from substorm growth to substorm expansion phase as observed with a radial configuration of ISTP and Cluster spacecraft, *Ann. Geophys.*, **23**, 1, 2005.
12. Shiokawa, K., I. Shinohara, T. Mukai, H. Hayakawa, and C. Z. Cheng, Magnetic field fluctuations during substorm-associated dipolarizations in the nightside plasma sheet around X=-10 RE, *J. Geophys. Res.*, **110**, A05212, doi:10.1029/2004JA010378, 2005.
13. Voronkov, I., E. F. Donovan, B. J. Jackel, and J. C. Samson, Large-scale vortex dynamics in the evening and midnight auroral zone: Observations and simulations, *J. Geophys. Res.*, **105**, 18,505, 2000.
14. Voronkov, I. O., Near-Earth breakup triggered by the earthward traveling burst flow, *Geophys. Res. Lett.*, **32**, L13107, doi:10.1029/2005GL022983, 2005.